# NONINVASIVE GLUCOSE SENSOR SYSTEM DEVELOPMENT: A STUDY OF NOISE SOURCES

Based on a research scholarship stay supported by
Austrian Marshall Plan Foundation


Zeinab Amin-Akhlaghi
Carinthia University of Applied Science
University of Iowa
Email: zibaam1@gmail.com


Advisor: Prof. David R. Andersen
March – August 2010

# Table of Contents

# 1 Abstract

An infrared glucose sensor studied, which is a part of continuous glucose monitoring system for diabetes. The sensor system consists of two infrared LEDs that shine the light on an interstitial fluid tube, an array of photo-diodes which detect the transmitted spectra, and a delta-sigma analog to digital converters. The system is capable of continuous data acquisition, and the sensor measures the concentration of glucose in the near infrared region, where glucose has absorption features. Various sources of noise are described, and a noise model studied that predicts the noise characteristics of the system. High signal-to-noise ratio is required for accurately quantifying the concentration of glucose, which is limited by the low luminosity and low impedance of the photodiodes. Finally the system performance and measurement described.

# 2 Introduction

Diabetes is one of the most common and conventional causes of death in industrialized countries. It is a condition of high blood sugar, either because of insufficient insulin, or weak response of cells to the insulin produced. According to the World Health Organization, at least 171 million people worldwide suffer from diabetes, or 2.8% of the world population, which is estimated to double by year 2030 [1]. Diabetes occurs throughout the world; however it is more commonly observed in some developed countries, such as US, Canada, Italy and Spain. Among the European countries Cyprus, Spain, Portugal and Austria have highest percentage of prevalence of diagnosed diabetes in the general population, which is about 6% of their population. The increase in diabetes incidence in developing countries follows the trend of lifestyle changes, perhaps most importantly a Western-style diet [1]. The patients are recommended to follow certain diet and exercises to keep their blood glucose levels within acceptable bounds. Yet developing of a continuous health care monitoring is a challenge.

Diabetes is the most common disorder of the endocrine (hormone) system, occurs when blood sugar levels in the body consistently stay above normal. Based on its cause, diabetes is categorized into two types: Either the body is unable to make insulin (type 1 diabetes) or the body does not respond to the effects of insulin (type 2 diabetes). Also it can also appear during pregnancy. Insulin is one of the main hormones, which regulates blood sugar levels and allows the body to use sugar (glucose) for energy.

To the best of our knowledge, the diabetes cannot be cured; however it can be treated and controlled. It is usually recommended that the patients manage their diabetes by:

- Keeping the blood sugar levels as near to normal as possible, by balancing food intake with diabetes medication and physical activity.
- Maintaining the blood cholesterol and triglyceride (lipid) levels as near their normal ranges as possible, by decreasing the total amount of fat to 30% or less of the total daily calories and by reducing saturated fat and cholesterol.
- Controlling the blood pressure, i.e. the blood pressure should not go over 130/80.
- Slowing or possibly preventing the development of diabetes-related health problems.

Moreover there are several habits that can help the patient to control their diabetes:

- Planning the diet following a balanced meal plan
- Exercising regularly
- Taking medicine, if prescribed, and closely following the guidelines on how and when to take it
- Monitoring the blood glucose and blood pressure levels at home
- Keeping appointments with the health care providers and having laboratory tests as ordered by the doctor

The most important factor is the regular home monitoring of glucose, which is not comparable to the check which doctors do every few months during the checkups. Recently, there have been efforts to develop continuous glucose monitoring systems, which are devices that continuously record blood sugar levels throughout a certain time period [2]. Self monitoring of blood glucose (SMBG) is an important method used to control diabetes [2][3]. Preventing of high or low blood sugar conditions together with using of artificial pancreas offer sort of cure for diabetes [2]. The so-called artificial pancreas consists of an insulin delivery pump, which is controlled using some type of glucose-sensing technology. As a response to detected changes in the blood glucose concentrations, the insulin is

continuously delivered. For such a system, the glucose sensing component must be able to provide an accurate and rapid blood glucose values to a microprocessor, which computes the amount of insulin required and then controls insulin delivery. The major limitation of a successful development of an artificial pancreas is the implantable glucose sensing technology and the electronic support required to control the instrumentation. One possible physical implementation of the glucose sensor is shown in
Figure 1.

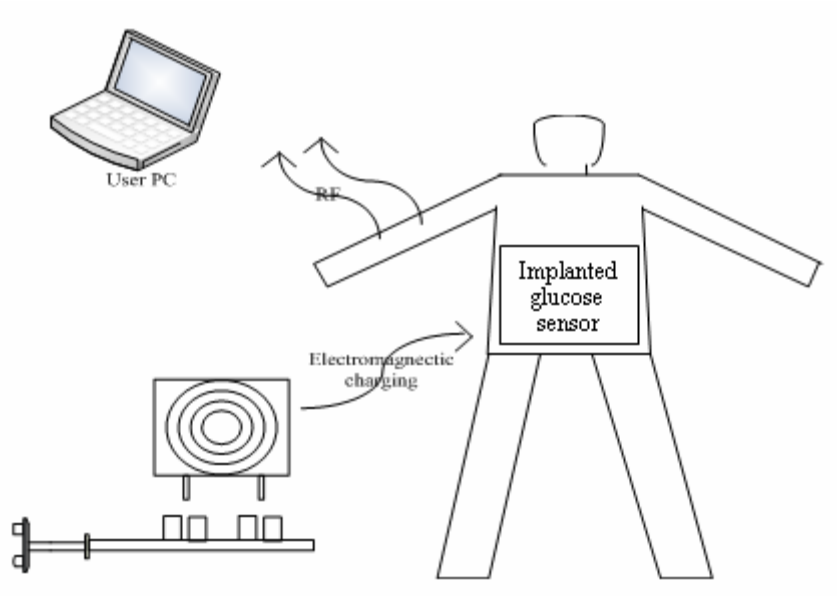


**Figure 1 Physical Implementation of the Glucose Sensor and Controller System [6]**

Among the research and development activities in this field, we can also mention the state-of-the-art Medtronic's MiniMed device that can provide up to 288 glucose measurements every 24 hours [5]. The system is used to measure an average blood sugar for up to 3 days, while the person with diabetes continues daily activities at home. In this approach a tiny glucose-sensing device is inserted under the abdomen skin, because the sensor should be in direct contact with the blood. The measured values are recorded each 5 minutes and should be monitored by patient.

Our project aims toward future miniaturization into an implantable, continuous glucose monitor. Unlike the commercially available device mentioned above, an implantable glucose monitor requires limited user intervention and does not require the cost of materials required for SMBG with finger-sticks [6]. We have decided to focus of the IR range of glucose absorption spectrum, since it has three pronounce peaks, shown in Figure 2 of reference [6]. Also we have considered a suitable IR photodetectors operates in the range of 2.2 μm to 2.4μm. The uniqueness of glucose spectrum is known in literature (Figure 2), where the concentration of glucose can be obtained from direct analysis of this spectrum [6].

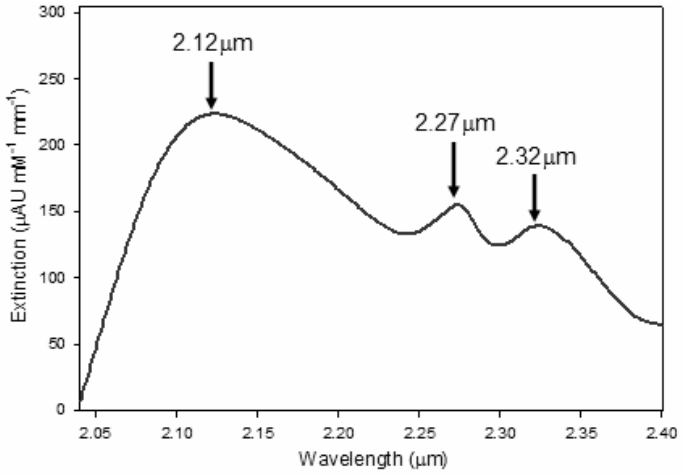


**Figure 2 Spectral uniqueness of glucose. IR Glucose absorption bands in near-IR region, and 3 indicated peaks. [6]**

In this paper, we study the noise effects in a developing low noise photocurrent measurement system. Various electronic parts of our system contribute in the total noise, hence reduces the signal to noise ratio (SNR). Major noise contributions are from transimpedance amplifiers (TIAs), photodiodes, and analog to digital converters (ADCs). The rest of this paper is organized in the following sections. Section 2 contains a project overview and details of the system; section 3 discusses the sources of noise, section 4 described the system performance, results and summary.

# 3 Project Overview

This project aims toward reduction of noise in an infrared glucose sensor system. The system comprises two LEDs which shine the light on a fluid tube, which can be either normal water or sweet water which represents the interstitial fluid. An array of 32 low shunt resistance IR photodiodes photo-detectors measure photocurrent generated by the transmitted light. Suitable TIAs are used to translate photocurrent from the photodiode array into voltages. A delta-sigma analog to digital converters (Δ-Σ ADCs) is applied to sample the input measurements in digital values. Usually, photodiodes are reverse biased to increase the bandwidth of the photoreceiver, while the IR photodiodes we utilize cannot be reverse biased due to the large reverse saturation current and low reverse saturation voltage. Our photodiodes have a low shunt resistance of 30 kΩ, which limits the SNR due to the noise properties of the TIA. Our IR photodiodes have relatively low photocurrent of 10 nA due to limited amounts of LED light reaching the linearly variable filter and the limited amount of luminous power transmitted through the filter to each photodiode. Lower photocurrent directly reduces the system SNR.

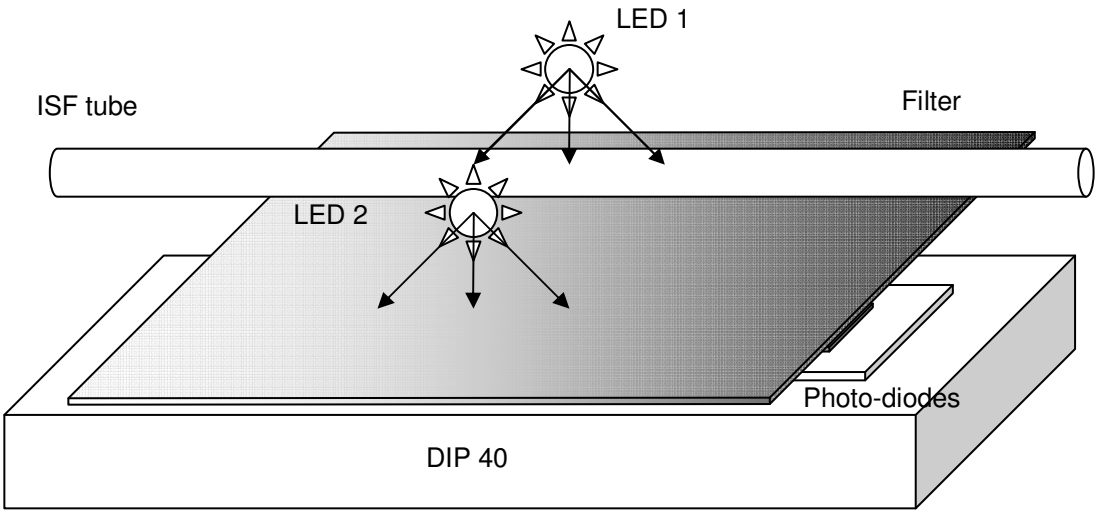


**Figure 3 Schematic view of the setup**

The glucose sensor measures the absorbance spectrum of glucose. IR light from LEDs is transmitted through analyte contained in a fluid chamber. As IR light of LED1 propagates through the interstitial fluid (ISF) sample, glucose absorbs a portion of the light near the peaks in the glucose absorption spectrum. Light from LED2 does not pass through the analyte on its way to the photodiodes. Photocurrent measurements with LED2 on are used to normalize the LED1 photocurrent data and compensate for temperature changes. We need measurements of the photocurrent with both LEDs off, LED1 on only, and LED2 on only to calculate the glucose concentration when the glucose sensor is used.

A linearly variable bandpass filter and a 32 element photodiode array form a spectrometer to measure the absorption spectrum. The photodiode array operates in the range of 2.2μm to 2.4μm where there are three peaks in the glucose absorption spectrum. The data acquisition unit (DAU) must measure the photocurrent from the photodiodes and provide glucose absorbance spectrum measurements at a frequency of 1 Hz on a continuous basis. Low noise metal film resistors are used to simulate the glucose sensor while evaluating noise characteristics of the DAU.

The Transimpedance Amplifier (TIA) is utilized to convert the low-level current to a proper voltage. The block diagram of such circuit is shown in Figure 4.

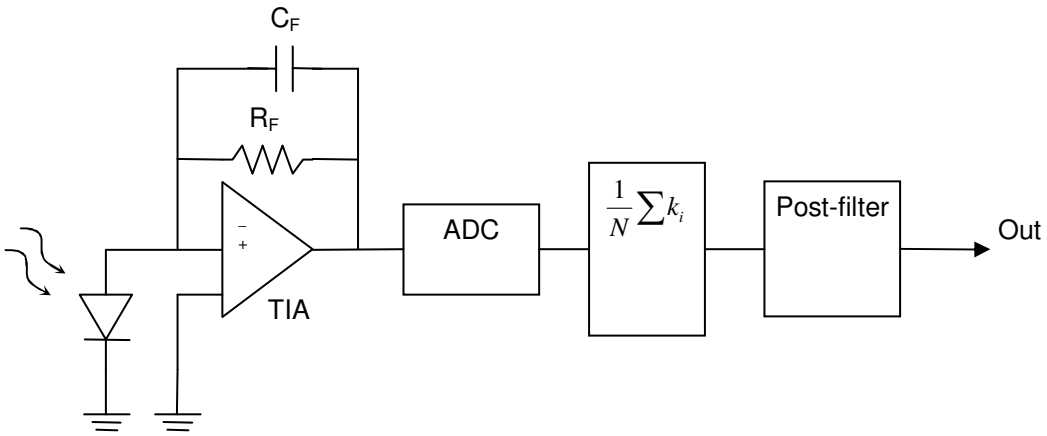


**Figure 4 Block diagram of the system, including photo diode, transimpedance amplifier, and other parts**

Figure 5 shows a photograph of the system, where one can see the position of photodiodes array, filter, ISF tube, etc. In this Figure, the LEDs are not visible, since they are mounted below the holder connected on a stand. Using this setup, we can change the position of the LEDs along 3 directions, and we try to optimize the position of LEDs to maximize the incident light on photodetector array.

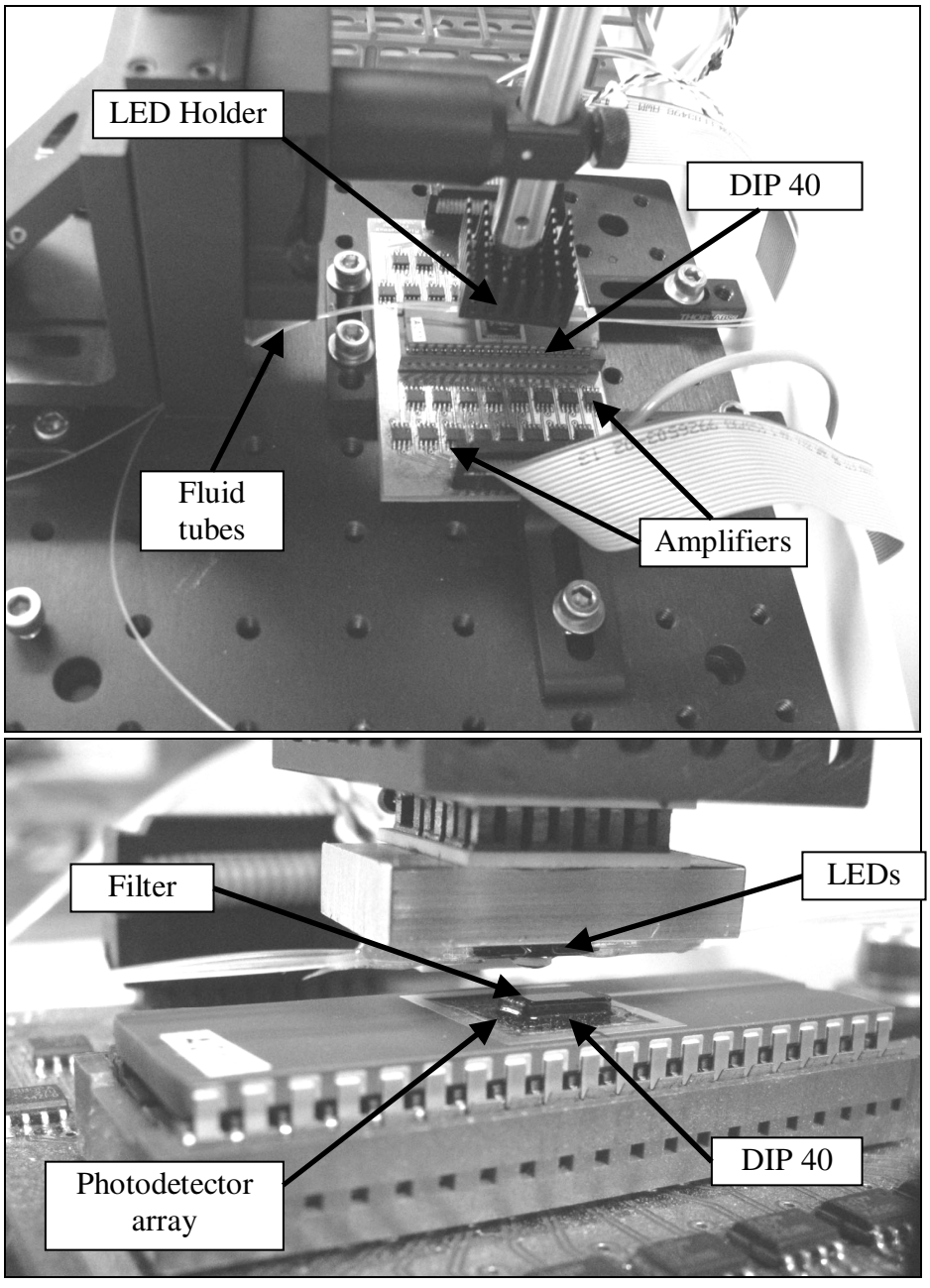


**Figure 5 Photographs of the setup, used to optimize the position of LEDs**

# 4 Sources of Noise and Filtering

In this chapter we study various sources of noise and filtering. We use the term noise to represent random electromagnetic fields occupying the same spectral region as that occupied by some signal. Random electrical noise is present in almost every type of component used in a circuit. This includes current or voltage noises in amplifiers, resistors, diodes, etc. The circuit designers are interested in various type of noise, including random electrical noise generated by the components, conducted noise through the power supplies that appear at the output due to finite PSRR, various sources of radiated emission pickup (EMI), micro-phonic effects due to system vibration, and high narrowband noise that is in fact a parasitic oscillation. In this project, we only consider the random electrical noise generated by the components themselves. The noise effect of all other components and external noises are not considered.

Figure 6 shows the noise analysis circuit of a TIA. This includes three equivalent input noise terms for the op amp and three resistor noise terms [11]. We consider that the elements around the op amp are purely resistive. Normally, reactive elements (capacitors, inductors and transformers) are considered to be noiseless, however they can strongly influence the frequency response for the noise generators in a circuit. The Johnson noise of the resistor may be represented as either a current or a voltage. It is shown that the total output spot noise voltage for any op amp at a selected frequency can be calculated as [11]

$$E_O = \sqrt{\left(E_{NI}{}^2 + (I_{BN}R_S)^2 + 4k_BTR_S\right)G_N{}^2 + (I_{BI}R_F)^2 + 4k_BTR_FG_N}$$

Here T is the temperature in Kelvin, $E_{NI}$ is Op Amp input noise voltage, $I_{BN}$ is the Op amp non-inverting noise current, $I_{BI}$ is the Op amp inverting noise current, $E_{RS} = \sqrt{4k_BTR_S}$ is

the source resistor noise voltage, $E_{RF} = \sqrt{4k_B T R_F}$ is the feedback resistor voltage and $I_{RG} = \sqrt{4k_B T / R_G}$ is the gain setting resistor current.

Once the complete output spot noise equation for an op amp is developed (above Equation), all other descriptions or simplifications may be derived. This equation is also important as what is actually being measured in any noise measurement.

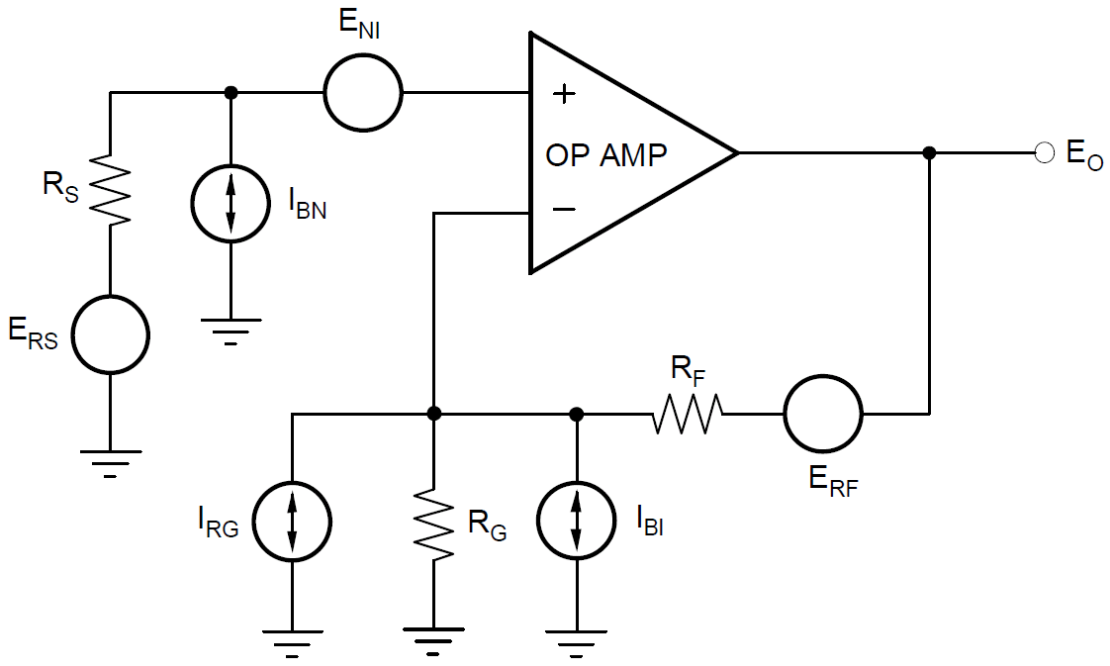


**Figure 6 Op Amp Noise Analysis Circuit** [11]

Another important factor which is included in the above mentioned equation is the effect of Johnson noise. As mentioned earlier, we are interested in the IR spectrum of Glucose where it has three absorption peaks. Therefore, we have chosen a photo-detector, intentionally designed by our colleagues [12] to cover the wavelength range of 2.1µm to 2.4µm. It is shown that III–V semiconductor alloy materials, such as GaInAsSb detectors are capable of showing the best performance and flat responsivity in this wavelength region (Figure 9 of

Reference [12]). But on the other hand, these materials have much lower resistance than typical Si-based photodetectors, and therefore the effect of Johnson noise is higher, which is inverse proportional to resistivity.

Johnson noise or thermal noise is the electronic noise generated by the thermal agitation of the charge carriers inside an electrical conductor at equilibrium, which happens regardless of any applied voltage. The thermal noise is almost white, i.e. the power spectral density is nearly equal throughout the frequency spectrum [13]. All resistors have a Johnson voltage noise of $v_J = \sqrt{4k_B T \Delta f R}$, or equivalently current noise of $i_J = \sqrt{4k_B T \Delta f / R}$ where $k_B$ is Boltzmann's Constant, $T$ is the absolute temperature, $\Delta f$ is the bandwidth, and $R$ is the resistance. It is clear that the smaller resistivity of GaInAsSb photodetectors results in higher current noise.

Including the ADC noise voltage ($\Delta V_{ADC}$) as well as positive and negative voltage reference noise ($\Delta V_{REF}$) we find a noise model for the TIA:

$$E_O = \sqrt{(E_{NI} G_N)^2 + (I_{BI} R_F)^2 + 4kTR_F G_N} \sqrt{+ \Delta V_{ADC}^2 / N + \Delta V_{REF}^2 + \Delta V_{REF}^2},$$

where N ADC samples are averaged per data point.

We calculate the SNR of the noise model using the expression

$$\text{SNR [dB]} = 10 \log_{10}(I_{PC} R_F / E_O),$$

where $I_{PC}$ is the photocurrent and $R_F$ is the feedback resistor. One multiplies the logarithm in above equation by 10 instead of 20 when calculating the SNR because the photocurrent is proportional to the luminosity of light arriving at the photodiode and luminosity is luminous power per unit area.

Another source of noise happens in ADC, and called quantization noise, which limits ADC's dynamic range. Oversampling and dithering are two methods for improving the quantization noise performance in practical ADC applications [14].

The fluctuation of measurements data can be used to calculate the show the total signal to noise ratio. Here, the experimental signal to noise ratio of the system can be defined as

$$SNR = \frac{\text{Voltage expected value}}{\sigma_{\text{exp}}} = \frac{I_{PD} \times R_F}{\sigma_{\text{exp}}}.$$

Here $\sigma_{\text{exp}}$ is the standard deviation of the measurements.

## 4.1 Circuit Design

A block diagram of the DAU is shown in Figure 7. A microcontroller provides LED1 and LED2 enable signals to turn the IR LEDs on and off. Photocurrent from the photodiode array is routed to the TIAs and the resulting voltages are sampled by the ADCs. Timing signals from the microcontroller determine when samples are recorded and sent to the microcontroller via the serial port. A low noise voltage reference is provided to the ADCs. Power conditioning circuitry generates and filters four voltages required by components of the DAU.

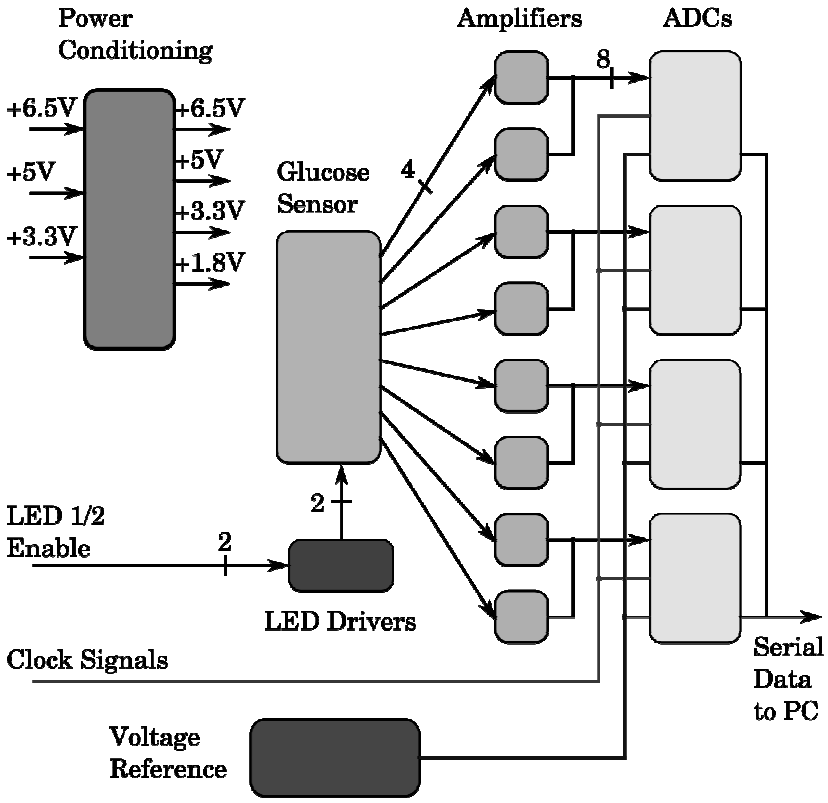


**Figure 7 Block diagram of the DAU [8]**

The circuit design used for each of the DAU's 32 channels is similar to the Figure 4. We compared noise performance of several op amps by combining shot noise on the offset current, op amp input current noise, and op amp voltage noise to select an op amp for the TIA. Here the offset current is the sum of the op amp input offset current and the current in $R_{PD}$ due to the op amp offset voltage. We included shot noise on the offset current since the source of the photodiode current is a diode junction. This calculation showed the MAX4478 [15] minimized the noise voltage for the components considered.

The chief factors affecting choice of the ADC are the resolution, ADC noise, conversion time, and ability to use a negative analog voltage source, $AV_{SS}$, of 2.5V below the digital ground. We also need a minimum of 20 bit resolution to keep the quantization error well

below the system noise. We chose the ADS1258 [16], a 24 bit Δ-Σ ADC with 16 single ended channels that allows $AV_{SS}$ of -2.8V with respect to DGND. The serial data out pin of this ADC can be tri-stated so just one serial port is required to record ADC samples. We need to measure photocurrent spectra with LED both LEDs off, LED1 on only, and LED2 on only to calculate glucose concentration. Since we measure photocurrent with both LEDs off twice we record 4 types of data samples 250 times a second, requiring a sample rate of 1 kHz. This is well below the ADS1258 maximum sample rate. We selected the ADR440 [17] for positive and negative voltage references because it has a very low noise voltage of 1.0 $\mu V_{p-p}$ and operates with only 0.5V dropout voltage.

## 4.2 Filtering

Transimpedance op amps are used as an analog filter to simplify the sensor input designs, and suitable feedback capacitor is chosen for stability and large bandwidth. Figure 8 shows a transimpedance amplifier circuit. A large-enough resistor of $R_F = 10^7 \Omega$ is chosen to convert the input current to a reasonable output voltage range. To stabilize the circuit, a large enough capacitor of $C_F = 10^{-9} F$ is placed in parallel with the feedback resistor. This ensures that the design has the largest possible bandwidth, and it is still be stable [10]. $I_{PD}$ is the current that occurs from the photodiode action. This circuit inserts a pole at $\omega = 1/C_F R_F$ and this pole stabilizes the circuit. For the selected values of $R_F = 10^7 \Omega$ and $C_F = 10^{-9} F$, the cutoff frequency becomes

$$\omega = \frac{1}{C_F R_F} = 100 \frac{Rad}{s} = \frac{100}{2\pi} Hz .$$

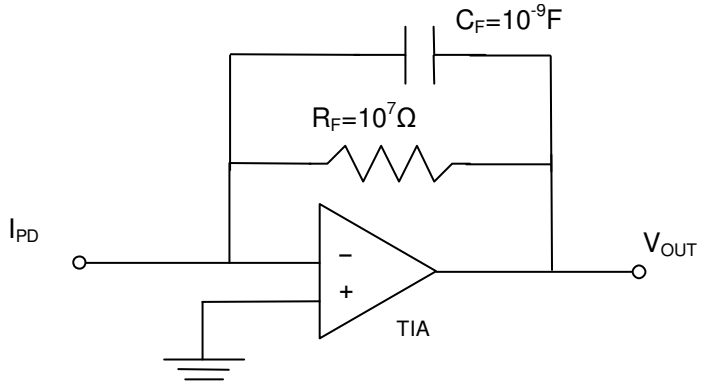


**Figure 8 Basic transimpedance amplifier configuration used as an analog filter**

In addition to the digital filter, it is necessary that we use the above mentioned cutoff implemented by the analog filter shown in Figure 8, whose function is to take the selected frequency region highlighted in Figure 9. This filter excludes the repetitions of several peaks and therefore we only consider the main highlighted peak.

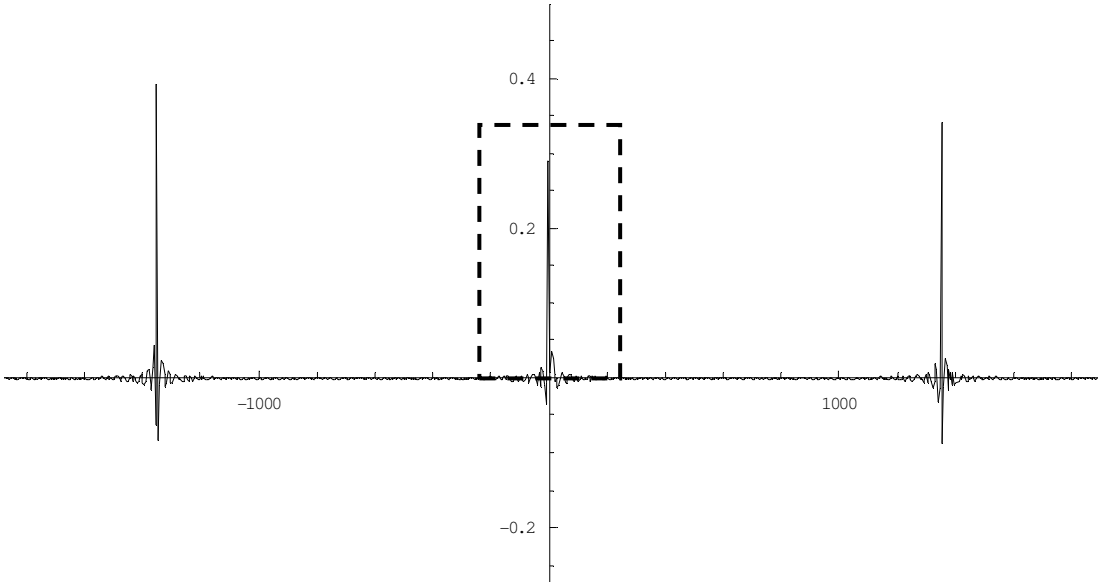


**Figure 9 Fourier transform of averaging filter.**

The moving average is the most common filter in DSP, mainly because it is the easiest digital filter to understand and use. In spite of its simplicity, the moving average filter is optimal for a common task: reducing random noise while retaining a sharp step response. This makes it the premier filter for time domain encoded signals. However, the moving average is the worst filter for frequency domain encoded signals, with little ability to separate one band of frequencies from another. Relatives of the moving average filter include the Gaussian, Blackman, and multiple-pass moving average. These have slightly better performance in the frequency domain, at the expense of increased computation time. [9]

The Butterworth filter is one type of signal processing filter design, which is designed to have a frequency response which is as flat as mathematically possible in the pass band. Therefore it is also called “maximally flat magnitude filter”. The Butterworth type filter was first described on 1930 by the British engineer Stephen Butterworth [1].

# 5 System Performance and Summary

In this project we verify the SNR of the DAU system by simulating the sensor with low noise metal film resistors with resistance equal to the photodiode shunt resistance and also with photodiode itself. The ADCs send the four types of photocurrent samples described above to the microcontroller which calculates the average of 215 samples to form one data point for each photodiode channel every second. We use the standard deviation of 1000 consecutive data points to calculate the SNR for a representative number of photodiode channels. Fig. 8 compares thermal noise, noise model, and experimental data from this research and a previous study on photocurrent measurement with low impedance photodiodes [14]. Fig. 8 shows that data from the present DAU design are comparable with results from [14] which used a current input ADC instead of our method with a TIA and voltage input ADC.

Various sources of noise vary with test resistivity. Therefore over each resistivity range, the total expected noise is dominated by one or two effects, shown in Figure 10. Here the higher total expected noise is equivalent to lower SNR.

From our experimental results, $I_{PC}$ is typically 10 nA. We chose a value of 10 MΩ for $R_F$ in order to yield a signal voltage of 0.1 V that is within the input range of the ADC. Figure 11 is a plot of the SNR for this noise model versus $R_T$ with N=215. We use N=215 since this number of samples are available from the ADC in one second and we require one data point per second. We show thermal noise in Figure 11 to indicate the maximum SNR possible if the op amps, ADCs, and voltage reference were ideal components. The graph of the noise model has three straight segments and a different term from (5) is dominant in each segment. The left segment has a slope proportional to $1/R_T$ and is due to the $E_{NI}$ term in (5). The middle segment has a slope proportional to $(R_T)^{-1/2}$ and is due to thermal noise from

$R_T$. Increasing $R_T$ improves the SNR. The final, flat section arises from the combination of noise from thermal noise of the feedback resistor ($E_{RF}$), input current noise ($I_{BI}$), $\Delta V_{ADC}$, and $\Delta V_{REF}$. Calculating these noise voltages with our final component values shows $\Delta V_{REF}$ provides the SNR limit within the right segment of Figure 10.

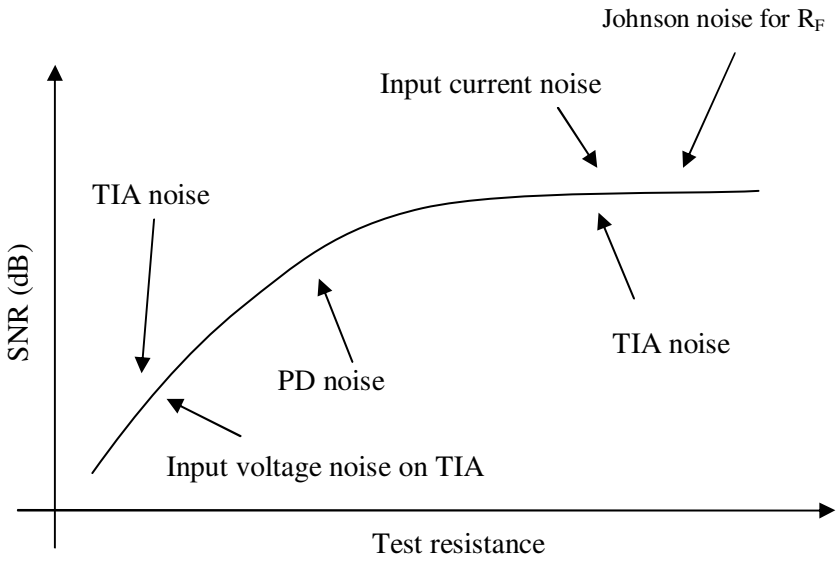


**Figure 10 Schematic diagram of total expected noise. Arrows show the areas where noise is dominated by each effect.**

Our method for measuring photocurrent using the TIA shows this method can provide improved SNR relative to previous efforts. Our experimental results show that an undesired noise source is present in the current design and we are working to identify and remove this noise source. A fan cooled the DAU to reduce the effects of thermal drift during our experiments. This is reasonable here since when the DAU and glucose sensor are designed into an implantable device the system will have lower power dissipation and be in a constant temperature environment.

Additional noise sources will be present when using actual glucose sensors with the DAU. The photocurrent and dark current would both provide shot noise since they originate from

a diode junction. In order to eliminate shot noise from dark current the photodiodes cannot be reverse biased. The shot noise from 10 nA of photocurrent is 57 fA. The voltage created by this current passing through $R_F$ is 0.57 µV. The noise model predicts approximately 48.1 dB of SNR with $R_T$ of 30 kΩ, which corresponds to 6.3 µV of noise voltage. Adding these two noise voltages still results in 48.1 dB SNR so the shot noise on the photocurrent will not significantly degrade the SNR.

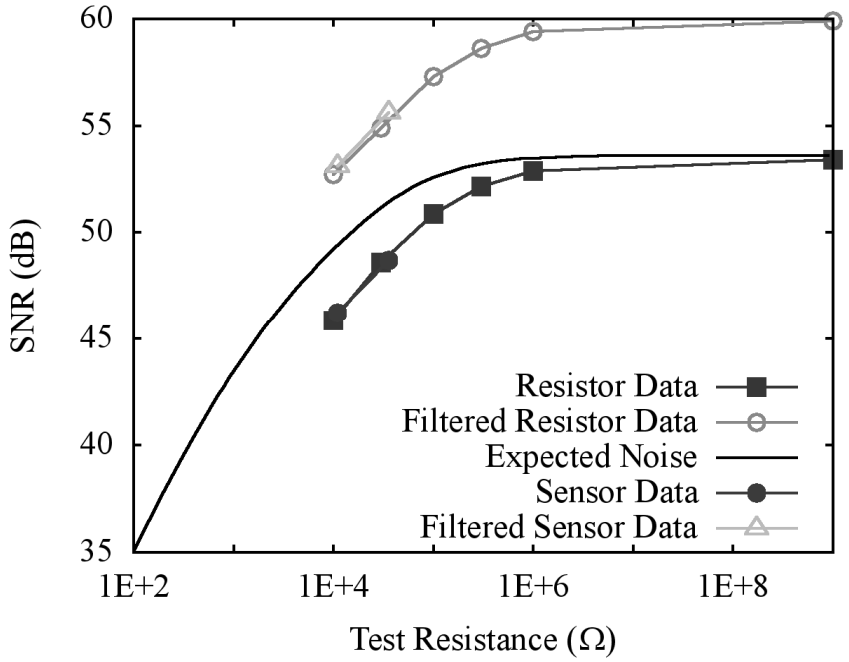


**Figure 11 Expected results from noise model and experimental data.**

Figure 11 is a summary plot of the SNR versus resistance data. Values for the metal-film resistors as well as for two different sensor photodiode arrays are shown. The results for the photodiode arrays agree nicely with the metal film results. The black curve indicates the SNR from our noise model. Resistor and Sensor results are those obtained with no digital filtering beyond our simple averaging technique (1 Hz data). Filtered results include a digital Butterworth filter with 0.025Hz bandwidth on the backend (same 1 Hz data rate).

We have good agreement with theoretical noise model for most values of $R_{PD}$. For smaller values of $R_{PD}$, there is some reduction in SNR from that predicted theoretically. This variation is due to small thermal changes in the TIA input offset voltage that gives rise to changes in photocurrent. This effect is most significant for small values of $R_{PD}$ and will be eliminated when the sensors is embedded in a constant temperature bath, e.g. the human body.

The DAU was designed using TIAs and Δ-Σ ADCs to measure the photocurrents from a 32 photodiode array in a specialized glucose sensor. We are presently beginning to integrate the DAU with glucose sensors to measure glucose concentration in glucose solutions and ISF. Subsequent research includes miniaturization of the sensor and DAU electronics into an implantable glucose monitoring system. The shot noise on the photocurrent will not significantly degrade the system noise characteristics when glucose sensors are used.

# 6 Conclusion

This scholarship visit has covered parts of a larger project in The University of Iowa, which is supported through American National Institutes of Health. During this part of the project, an infrared glucose sensor studied, which is a part of continuous glucose monitoring system for diabetes. The sensor system consists of two infrared LEDs that shine the light on an interstitial fluid tube, an array of photo-diodes which detect the transmitted spectra, and a delta-sigma analog to digital converters. The system is capable of continuous data acquisition, and the sensor measures the concentration of glucose in the near infrared region, where glucose has absorption features.

As a part of development process of the noninvasive glucose sensor system, this project is focused on the describing various sources of noise and studying the noise model that predicts the noise characteristics of the system. High signal-to-noise ratio is required for accurately quantifying the concentration of glucose, which is limited by the low luminosity and low impedance of the photodiodes. Finally the system performance and measurement described. Further development of the noninvasive glucose sensor system includes the optimizing the position of LED and photodetectors, and minimizing the total size of the system.

## Acknowledgement

Zeinab Amin-Akhlaghi thanks Marshall Plan Foundation for granting the scholarship. She also thanks Daniel W. Cooley and Prof. David R. Andersen from Department of Electrical and Computer Engineering, and Department of Physics and Astronomy, The University of Iowa, Iowa City, Iowa for numerous supports. The whole project in University of Iowa is supported through American National Institutes of Health (NIH) Grant No. DK064569.

# References

[1] S. H. Wild, G. Roglic, A. Green, R. Sicree, and H. King, "Global prevalence of diabetes: estimates for the year 2000 and projections for 2030." vol. 27: Am Diabetes Assoc, 2004, p. 2569.

[2] C. W. Chia and C. D. Saudek, "Glucose sensors: toward closed loop insulin delivery," *Endocrinol. Metab. Clin. N. Am.*, vol. 33, pp. 175-195, 2004.

[3] C. D. Saudek, R. L. Derr, and R. R. Kalyani, "Assessing Glycemia in Diabetes Using Self-monitoring Blood Glucose and Hemoglobin A 1c," *JAMA*, vol. 295, pp. 1688-1697, 2006.

[4] Life Extension Writings by Ben Best, http://www.benbest.com/lifeext/causes.html

[5] WebMD, Diabetes Health Center, http://diabetes.webmd.com/continuous-glucose-monitoring

[6] K. Kanukurthy, U. Viswanathan, D. R. Andersen, J. Olesberg, M. A. Arnold, and C. Coretsopoulos, "Controller for a continuous near infrared glucose sensor," 2005, pp. 59-65.

[7] S. Butterworth, "On the Theory of Filter Amplifiers.'", 1930, pp. 536-541.

[8] D. W. Cooley and D. R. Andersen, "Low Noise Measurement of Photocurrent From Low Impedance Photodiodes", in IEEE EIT2010, IEEE International Conference on Electro/Information Technology, Normal, IL, USA, 2010

[9] The Scientist and Engineer's Guide to Digital Signal Processing By Steven W. Smith, Ph.D., http://www.dspguide.com/ch15.htm

[10] Understand and apply the transimpedance amplifier, http://www.mobilehandsetdesignline.com/201400084

[11] M. Steffes, "Noise Analysis for High-Speed Op Amps", Application Report, Texas Instruments

[12] M. H. M. Reddy, J. T. Olesberg, C. Cao, and J. P. Prineas, "MBE-grown high-efficiency GaInAsSb mid-infrared detectors operating under back illumination." vol. 21: IOP Publishing, 2006, p. 267.

[13] J. B. Johnson, "Thermal agitation of electricity in conductors." vol. 32: APS, 1928, pp. 97-109.

[14] R. Lyons and R. Yates, "Reducing ADC quantization noise." vol. 44: Penton, 2005, pp. 72-80.

[15] MAX4478 datasheet (www.maxim-ic.com).

[16] ADS1258 datasheet (www.ti.com)

[17] ADR440 datasheet (www.analog.com ).